



# Streamflow drought: implication of drought definitions and its application for drought forecasting

Samuel J. Sutanto<sup>1</sup> and Henny A. J. Van Lanen<sup>1</sup>

<sup>1</sup>Hydrology and Quantitative Water Management Group, Environmental Sciences Department, Wageningen University and Research, Droevendaalsesteeg 3a, 6708PB, Wageningen, the Netherlands

**Correspondence:** Samuel Sutanto (samuel.sutanto@wur.nl)

**Abstract.** Streamflow drought forecasting is a key element of contemporary Drought Early Warning Systems (DEWS). The term streamflow drought forecasting, rather than streamflow forecasting, however, has created confusion within the scientific hydro-meteorological community, as well as in operational weather and water management services. The way, how streamflow drought is defined, is the main reason for this misperception. The purpose of this study, therefore, is to provide a comprehensive overview of the differences within streamflow droughts using different identification approaches for European rivers, including an analysis of both historical drought and implications of forecasting of these extreme events. Streamflow data were obtained from a LISFLOOD hydrological model forced with gridded meteorological observed (known as LISFLOOD-Simulation Forced with Observed, SFO). The same model fed with seasonal meteorological forecasts of the European Centre for Medium-range Weather Forecasts system 5 (ECMWF SEAS 5) was used to obtain the forecasted streamflow. Streamflow droughts were analyzed using the Variable Threshold (VT), Fixed Threshold (FT), and the Standardized Streamflow Index (SSI). Our results clearly show that streamflow droughts derived from different approaches deviate from each other both in occurrence and timing, associated with different climate regions across Europe. The occurrence of FT drought is higher than droughts based upon VT and SSI, which highlights the importance of seasonality. FT drought happens earlier in the year than droughts obtained from VT and SSI. The use of aggregating daily streamflow data into monthly time windows for forecasting drought, such as the application of 30-day Moving Average (30DMA), is recommended to identify the VT and FT droughts. This approach will eliminate the undesired minor drought events, which are identified when using non-aggregated daily flow data. There is no unique hydrological drought definition that fits all purposes, hence developers of DEWS and end-users should clearly agree among themselves upon a sharp definition on which type of streamflow drought is required to be forecasted for a specific application.



## 1 Introduction

Drought is a creeping natural disaster that has major socio-economic and environmental impacts across the world (e.g., Tallaksen and Van Lanen, 2004; Wilhite et al., 2007; Ding et al., 2011; Van Dijk et al., 2013; Stahl et al., 2016; Haile et al., 2019). IPCC (2014) reports with very high confidence that impacts from among others drought on society are already considerable.

25 Drought hazard and its impacts are projected to increase in numerous regions under a future warmer climate (e.g., Feyen and Dankers, 2009; Forzieri et al., 2014; Prudhomme et al., 2014; Wanders et al., 2015; Samaniego et al., 2018). Gu et al. (2020) analyzed how drought influences regional gross domestic product (GDP) under different representative concentration pathways (RCPs) and shared socioeconomic pathways (SSPs) at global scale. The fraction of drought-affected GDP relative to the country's GDP would equal 100% in over about 75 countries under 1.5°C warming, which is projected to increase to over

30 90 countries under 2.0°C warming. There is an urgent necessity for society to respond to these signs. National drought policy plans should be implemented that convert the usually reactive drought crises management into a pro-active risk management (Sivakumar et al., 2014; WMO and GWP, 2014; Poljanšek et al., 2017). One of the elements to be included is a Drought Early Warning System that in addition to real-time monitoring contains operational drought forecasting with appropriate lead times (i.e. multi-months or seasonal).

35 The term drought forecasting has been used in an indefinite way, which has created misconceptions, miss-citations, and confusion in the scientific hydro-meteorological community (authors, readers, editors, and reviewers), as well as in operational weather and water management services. An explicit definition what is being forecasted is crucial to avoid any misunderstanding on usability of drought forecast products for different purposes. Firstly, meteorological drought forecast systems have been developed (e.g., Mishra and Desai, 2005; Belayneh et al., 2014; Dutra et al., 2014), which use the Standardized Precipitation

40 Index, SPI (McKee et al., 1993) or the Standardized Precipitation Evaporation Index, SPEI (Vicente-Serrano et al., 2010). These aggregate precipitation (SPI) and precipitation minus evaporation (SPEI) over at least one month and have lead times of several months. Conventional weather forecast systems that predict low or no precipitation and above normal temperature, as part of their suite of forecast products, should be not classified as a drought forecasting system because of their rather short lead time (sub-daily to 10-15 days). Secondly, hydrological drought forecasts are provided (e.g., Pozzi et al., 2013; Sutanto et

45 al., 2020a), which involve groundwater, river flow, soil moisture, and runoff. Hydrological drought deviates from meteorological drought (e.g., Changnon, 1987; Peters et al., 2003; Mishra and Singh, 2010; van Loon and Van Lanen, 2012; Barker et al., 2016; Sutanto et al., 2020b), which means that the latter cannot straightforwardly used to predict drought in groundwater or river flow. Because of all these differences, an explicit delineation of what is being forecasted is prerequisite. Here, our study focuses on hydrological drought forecasting, specifically of drought in the river (streamflow drought), which is defined

50 as below-normal streamflow (Hisdal et al., 2004; Peters et al., 2006; Fleig et al., 2006; Feyen and Dankers, 2009; Sarailidis et al., 2019).

Forecasting of streamflow drought follows different approaches on how the hydrological drought is defined (Hisdal et al., 2004; van Loon, 2015), which is also essential to consider when using forecast products. Yuan et al. (2017) use the so-called standardized approach. They calculated the Standardized Streamflow Index (SSI), which measures monthly normalized



55 anomalies in streamflow and, if negative, then SSI signifies a dry anomaly. Others applied the threshold approach to derive  
drought in river flow from the forecasted flow time series. This implies that the river is in drought when it is below a predefined  
flow. Marx et al. (2018) and Wanders et al. (2019) use a fixed threshold meaning that it does not vary throughout the year.  
Usually, a percentile of the flow duration curve is taken using all flow data to identify the fixed threshold. In contrary, Fundel et  
al. (2013), Sutanto et al. (2020a), and van Hateren et al. (2019) have used the variable threshold approach to identify drought  
60 events with their hydrological drought forecasting system. In this approach the threshold varies over the year and accounts for  
seasonality, which means that drought can occur in every season. The threshold is derived from, for instance, the daily, monthly  
or seasonal flow duration curve.

In the context of this study, it is also important to realize, that hydrological drought forecasting is different from just stream-  
flow forecasting (e.g., Day, 1985; Clark and Hay, 2004; Schaake et al., 2007; Bell et al., 2017; Mendoza et al., 2017; Arnal  
65 et al., 2018; Duan et al., 2019), although the latter provides key input data to derive hydrological drought. For hydrological  
drought forecasting, an additional step is required, that is, derivation of drought events from the forecasted flow time series,  
e.g. the flow time series is converted in a time series of drought events. In summary, the different approaches that are being  
used to communicate drought in rivers call for an explicit description of what is being meant.

The purpose of this study, therefore, is to provide a clear overview of the differences between streamflow drought using  
70 different definitions. This is done through a historic analysis using data from 1990-2018. Differences are illustrated for the  
entire Europe and some major rivers across different climate regions. The historical analysis is innovative because it covers the  
entire pan-European river network with all its hydrological regimes instead of a country (Heudorfer and Stahl, 2017; Vidal  
et al., 2010) or a river basin (Sarailidis et al., 2019) and involves both threshold and standardized identification approaches.  
Eventually, its implications for forecasting hydrological drought are elaborated using the extreme 2003 drought in Europa as  
75 an example, which demonstrates that there no one fits all hydrological drought forecast. The observed and ensemble forecasts  
of streamflow datasets, used in this study, are described in Section 2.1, followed by a description of the methodology to derive  
the drought indices (Section 2.2). The results are presented and discussed in Section 3. Finally, we conclude the findings in  
Section 4.

## 2 Data and Methods

### 80 2.1 Data

A state-of-the-art hydrological model, LISFLOOD, was used to simulate the streamflow of rivers across Europe from 1990 to  
2018, which was derived from the routed runoff of 5 x 5 km grid cells (van der Knijff et al., 2010; Burek et al., 2013a). We  
decided to use simulated river flow rather than observed flow, because sufficiently-long times of observed flow for a common  
period covering the whole of Europe do not exist. The LISFLOOD model was fed by gridded meteorological observations  
85 (e.g., precipitation, temperature, relative humidity, wind speed) to obtain daily proxy for observed streamflow data, known  
as LISFLOOD-Simulation Forced with Observed (SFO). The gridded meteorological observation data were collected from  
ground observations (>5000 synoptic stations), obtained from the Joint Research Center (JRC) meteorological database, the



Global Telecommunication System of the WMO, and high-resolution data received from the National member States institutions (Pappenberger et al., 2011). The time series of proxy observed streamflow data for each cell at the river network across Europe were used to derive the streamflow drought following different approaches. Potential evapotranspiration was calculated through the offline LISVAP pre-processor based on the Penman-Monteith equation (van der Knijff, 2008; Burek et al., 2013b). A kinematic wave approach was used for routing the water movement on the river network. The model was calibrated using time series of observed river streamflow from over 700 calibration stations across Europe. The hydrological skill of the LISFLOOD model expressed by the Kling-Gupta Efficiency (KGE) shows that 42% of all calibration stations score a KGE higher than 0.75, 33% of all stations score a KGE between 0.5 and 0.75, and 25% of all stations score a KGE below 0.5 (Arnal et al., 2019). Although the model was originally developed for operational flood forecasts in the EU under European Flood Awareness System (EFAS) platform (Thielen et al., 2009; Pappenberger et al., 2011; Cloke et al., 2013), the LISFLOOD model has been tested for drought identification, forecasting and projections (Feyen and Dankers, 2009; Trambauer et al., 2013; Forzieri et al., 2014; Sutanto et al., 2019, 2020a, b; van Hateren et al., 2019). It appears that the model also performs rather well for drought studies. The model used in this study is the latest version of LISFLOOD that has been implemented in the operational EFAS since 2019 (version 3).

Besides the SFO data, we also used re-forecasted (known as hindcast) time series of streamflow data for the year 2003, as an example of drought forecasts. The European Centre for Medium-range Weather Forecasts System 5 (ECMWF S5) seasonal forecast was used as forcing for the LISFLOOD hydrological model to forecast streamflow at the pan-European scale (Stockdale et al., 2018). The seasonal forecasts are available as re-forecast data for each month from day 1 to day 215 (7 months lead-time) for 25 ensemble members (see Sutanto et al. (2020a) for detailed information). In this study we selected the re-forecast data from 2003, because a severe drought across extended areas in Europe was observed (Fink et al., 2006; Ionita et al., 2017; Laaha et al., 2017).

## 2.2 Streamflow drought identification

In this study, we employed two well-known drought identification methods, i.e. the threshold drought approach and the standardized drought approach (van Loon, 2015). Firstly, drought was derived from time series of streamflow data from 1990 to 2018 and re-forecasted data 2003 using the threshold-based approaches to indicate water deficit in different domains of the water cycle, in our case it is the surface water domain, i.e. determination of streamflow deficit. This threshold approach originates from the theory of runs and is developed based on a pre-defined variable threshold level (Yevjevich, 1967; Hisdal et al., 2004). The threshold approach uses an event-based sampling of the flow time series to convert this into a time series of drought events. The drought event starts when the hydrological variable falls below the threshold value and ends when it equals or rises above the threshold value. In this study, we applied two different types of drought threshold approaches, which are the Fixed Threshold (FT drought) and the Variable Threshold (VT drought). FT uses a pre-defined threshold, which is constant over the year and unique for each river grid cell. The VT varies in each day for each river grid cell. The VT method gains more popularity because this method considers streamflow seasonality in the dataset (Hannaford et al., 2011; Prudhomme et al., 2011; van Loon, 2015). Thresholds in this study were derived from the 90<sup>th</sup> percentile of the streamflow (Q90), which are



the flows that are equaled or exceeded 90 percent of the time. The Q90 was considered as drought threshold because most of the rivers across Europe are classified as perennial rivers. Moreover, the Q90 threshold lays within the range of the 70<sup>th</sup>-90<sup>th</sup> percentile that is commonly used in drought studies (Tallaksen et al. , 1997; Hisdal et al. , 2004; Fleig et al., 2006; Wong et al. , 2011). Using the Q90, means that fewer drought events are identified compared with higher thresholds, e.g., Q70 and Q80.

A backward 30-day moving average (30DMA) method was employed to the daily streamflow data as well as to the VT threshold to reduce the number of minor droughts (pooling procedure) (Fleig et al., 2006; van Loon and Van Lanen , 2012; Sarailidis et al., 2019). This means that we were moving averaged the first 30 days of the SFO data (from 1 to 30 January 1990) to calculate the streamflow on 30 January 1990. For the 31 January 1990, we were moving averaged the SFO data from 2 January 1990 to 31 January 1990 and so on until 31 December 2018. Missing 30DMA streamflow data from 1 to 29 January 1990 were not relevant since we have started drought analyses from the hydrologic year 1991 (from October 1990 to September 1991) to the hydrologic year 2018 (from October 2017 to September 2018). We applied the same hydrologic year for all European rivers. The reason for choosing the same hydrologic year is to ensure consistency in the analysis at the European level. For the threshold, we calculated the daily threshold values using the original streamflow data without applying 30DMA for each day (365 and 366 thresholds for no leap and leap years, respectively). The threshold values are the same for every year from 1990 to 2018. We then applied the backward 30DMA method to these daily threshold values and simply neglected the first 30 days threshold (1 to 29 January 1990) for the same reason as above. We also applied 30DMA to the forecast data. To handle the forecast streamflow data at the start of the 215 day forecasts, we moving averaged 29 days of preceding observed data (SFO) with one day of forecast to predict a possible drought event on the first day. For the second forecast day, we moving averaged 28 days of preceding observed with two days of forecast and so on. For example, the 30DMA forecasted streamflow on 1<sup>st</sup> August 2003 was obtained from moving averaging the SFO data from 3 July to 31 July 2003 with the forecasted streamflow on the first day (1 August 2003 lead time one day). Hence, the first 29 forecasted streamflow data from the 215 day time series include some observed flow.

Secondly, the Standardized Streamflow Index (SSI, Nalbantis and Tsakiris , 2009; Vicente-Serrano et al., 2012) was used to indicate drought in the river. The SSI was calculated using the same theoretical background as the Standardized Precipitation Index (SPI, McKee et al., 1993). The SSI calculation for any river grid cell was based on a monthly average streamflow record that is fitted to a gamma distribution, which is then transformed into a normal distribution so that the median SSI for the site and desired period is zero. Please keep in mind that the 30DMA method was not applied for SSI analysis since SSI uses monthly average streamflow data. We decided to use the gamma distribution as general distribution for the whole Europe since it can be used for hydrological forecasting of both high and low flows (Slater and Villarini , 2018) and none of single distributions fit all streamflow time-series across Europe (Vicente-Serrano et al., 2012). A 6-month accumulation period was used in this study to avoid many minor drought events (SSI-6 drought), following studies from Trambauer et al. (2015) and Barker et al. (2016). SSI with 1-month accumulation period (SSI-1 drought) was added only for comparison with SSI-6 to prove the aforementioned reason (Fig. 5 and Appendix Figures). Negative SSI values indicate a drought event, which means that the streamflow in a certain month (accumulation of average streamflow data for six months for SSI-6, incl. five preceding months) is lower than median streamflow of that month (median accumulation of average streamflow data for six months for SSI-6)



and vice versa for positive SSI values. To forecast the SSI-6 for a lead-time of  $x$ -month ( $x = 1, 2, \dots, 7$  months), we combined SFO data with forecast data, as introduced by Yuan et al. (2013) and Dutra et al. (2014). For example, the forecasted SSI-6 for August 2003 with 1-month lead-time (forecasts issued on 2<sup>nd</sup> August 2003) was estimated by combining the SFO data from March to July 2003 (five months) with August 2003 forecast data (one month). To forecast the SSI-6 for September 2003 with 2-month lead-time (forecasts issued on 2<sup>nd</sup> August 2003), we combined the SFO data from April to July 2003 (four months) with forecast data for August and September 2003 (two months), and so on for the rest. The drought event was categorized into four classes, which are: (i) mild drought:  $0 > SSI \geq -1$ , (ii) moderate drought:  $-1 > SSI \geq -1.5$ , (iii) severe drought:  $-1.5 > SSI \geq -2$ , and (iv) extreme drought:  $SSI < -2$  (Nalbantis and Tsakiris, 2009). Similar to the threshold approach, the standardized method uses an event-based sampling of the flow time series to convert this into a time series of drought events for further analysis.

### 2.3 Köppen-Geiger climate classification

The Köppen-Geiger climate classification has been built based on observed global temperature and precipitation data (Peel et al., 2007). There are four main climate types found in Europe, which are cold (D), arid (B), temperate (C) and polar (E). Each climate type can be classified into several sub-climate types. In our study area, the dominant sub-climate types are Bsk, Csa, Cfa, Cfb, Csb, Dfc, Dfb, Dsa, Dfa, Dsc, and ET (Fig. 1). In addition to the analysis of streamflow drought in all grid cells of the pan-European river network, four different rivers located in the major climate regimes of Europe were selected (Cfb, temperate oceanic climate; Dfb, warm-summer humid continental climate; Dfc, subarctic climate; and Bsk, Mediterranean climate). The locations of the selected rivers are as follow: 1) Rhine River near Cologne, Germany, located at 50.9°N and 6.9°E (Cfb), 2) Danube River near Budapest, Hungary, located at 46.9°N and 18.9°E (Dfb), 3) Kemijoki River near Kemi, Finland, located at 65.8°N and 24.6°E (Dfc), and 4) Ebro River near Asco, Spain, located at 41.2°N and 0.6°E (Bsk). The four rivers are indicated by red dots in Figure 1. For detailed information about climate classifications used in the study, see the Köppen-Geiger climate classification presented in Peel et al. (2007).

## 3 Results and discussion

We present the differences of streamflow droughts identified using different definitions in two parts. The first part provides results and discussion of the historical analysis that consists of the investigation of differences between drought analyzed using different approaches, in terms of occurrences and timing in river grid cells at the pan European scale, and four selected river basins (Section 3.1). The second part elaborates an example of the implication of streamflow drought forecasts using different definitions in one of the selected river basin (Section 3.2).



### 3.1 Historic analysis

#### 185 3.1.1 Streamflow drought occurrences

One of the most profound differences among streamflow drought using different indices is the occurrence of these events. Based on the definition, streamflow drought may be absent, or occur once or more in a hydrological year in a certain river grid cell. This happens when the streamflow falls below the thresholds (VT and FT) or when it is lower than median streamflow (SSI). Streamflow drought might occur every year (28 events), but this is rare, as shown in Figure 2a (VT). In some regions, especially in cold regions, such as in northern Europe and Alps, the occurrence of VT droughts exceeds 28 events during the study period. However, in most river grid cells across Europe (96% of all river grid cells), occurrence of VT drought is less than 28 events. The number of FT drought is in general higher than of VT droughts. In more than 50% of all river grid cells, the frequency of FT drought is higher than VT drought, which especially applies to the cold regions (Fig. 2b). In these cold regions, drought occurs not only during summer or autumn due to below-normal precipitation and higher evapotranspiration, but also during winter and spring seasons, depending on the length of the frost period and the timing of the snow incident, accumulation and melting (cold snow season drought) (van Lanen et al., 2004; Pfister et al., 2006; van Loon and Van Lanen, 2012). A warm snow season drought may also occur during spring or summer, associated with no snow occurrence during winter or earlier snowmelt than normal (van Lanen et al., 2004; van Loon et al., 2010). This causes an early peak in streamflow, resulting in lower streamflow in late spring and summer. van Loon and Van Lanen (2012) discuss in detail these types of drought events. In general, the number of SSI-6 drought is similar to VT, i.e. in 91% of all grid cells the occurrence is lower than 28 events.

VT and FT droughts also occurred more than once a year in some rivers flowing from Spain to Portugal that might be caused by minor drought events (>30 events, red color Fig. 2a and 2b). Minor drought events are also the main reason for high occurrence of FT droughts in the UK and west Europe (>30 events), such as France and Germany (Fig. 2b). Here, the FT threshold is larger than the VT threshold in the dry season (summer), which causes a higher number of periods with streamflow falling below the threshold. For example, the average VT threshold during summer in the Loire River France, close to Angers city, is 145 m<sup>3</sup>/s, which is lower than the FT threshold (219 m<sup>3</sup>/s). The higher occurrence of FT droughts in the regions' border with west Russia is also caused by minor drought events that occur during winter. In this season, the VT threshold, e.g. in the Daugava River in Minsk (81 m<sup>3</sup>/s), is lower than in summer due to lower streamflow during cold period in winter (112 m<sup>3</sup>/s). A different number of drought occurrences between VT and SSI-6 is clearly seen in Ireland (Fig. 2a and 2c, 100% and 65% of all Irish river grid cells have less than 28 events, respectively). In this region, the number of SSI-6 drought events is similar to FT drought, which is in some cases more than 30 events. SSI-1 (hydrological drought index if only one month of accumulation is considered), on the other hand, gives higher drought occurrence (>55 events in Ireland) than other approaches (VT, FT, and SSI-6) as been shown in Figure A1 (Appendix). This is plausible due to the occurrence of more drought events when the monthly streamflow drops below the median monthly flow.

215 In this study, we highlight the occurrence of minor droughts derived with the threshold methods especially the FT method as a causative factor for high drought occurrence in certain regions. A high number of minor droughts with short duration and small deficit volume may disturb drought analysis. Tallaksen et al. (1997) and Fleig et al. (2006) suggest several pooling procedures



to reduce the number of minor droughts, such as applying the inter-event time method, the moving average procedure, and the sequent peak algorithm. In addition to these techniques, exclusion of drought event with duration shorter than a given number of days is recommended (Jakubowski and Radezuk , 2004; van Loon et al. , 2012). For example, van Loon et al. (2012) excluded drought that has duration less than three days. In this study, although we excluded many minor drought events by applying moving average procedures, which is the 30DMA for drought analyses (Section 2.2), a few minor drought events are still visible (short drought event). A clear example of the exclusion of minor drought events by using the 30DMA approach can be seen in Figure 4 that will be discussed later in the Section 3.1.3 and 3.1.4.

### 225 3.1.2 Timing of streamflow drought

To investigate the timing of streamflow drought, we present the month when drought mostly started in each grid cell of European rivers (Fig. 3). The timing was determined for each drought event in the period October 1990 to September 2018 (coincides with hydrologic years in most of Europe). Figures 3a, 3b, and 3c indicate that there is a strong relation between streamflow drought timing in the rivers and the Köppen-Geiger climate regions across Europe (Fig. 1). In general, rivers located in the cold climate regions Dfc and ET (subarctic climate and tundra climate, respectively), such as in northern Europe and Alps, experience early streamflow drought events in early winter for FT drought, and between late winter and early spring for VT drought and SSI-6. Rivers located in Dfb regions (warm-summer humid continental climate), such as in central and east Europe, have a broad range of timings from winter to summer, which means that we could not distinguish between drought identification approaches. The timing of drought for the remaining climate regions (Cfb: temperate oceanic climate, Csb: warm-summer Mediterranean climate, Csa: hot-summer Mediterranean climate, and Bsk: cold semi-arid climate) is in the summer for FT drought and later for VT drought, i.e. around summer to early winter. In these climate regions, the distinction between FT drought (Fig. 3b) on one hand, and VT (Fig. 3a) and SSI-6 (Fig. 3c) droughts on the other hand is obvious. The timing for FT drought in these regions shows that drought occurs usually during summer. In 83% of all river grid cells in the Cfb, Csb, Csa and Bsk climates, the FT drought occurs in the months June, July and August. However, if we take into account the seasonality, as in the VT and SSI-6 approaches, the drought does not have to occur during the dry period. VT drought only starts to occur in the dry season when the river is low for a sustained period. VT and SSI-6 droughts appear mostly in autumn (Vidal et al. , 2010). On the other hand, the Standardized Streamflow Index with shorter accumulation period (SSI-1 drought) has earlier drought timing, which is in several grid cells in spring and summer (in 42% of all river grid cells, see Figure A2).

Rivers flowing through different climate regions and associated seasonality are affected by different VT and SSI-6 drought timings, e.g. the Rhine River flowing from Switzerland, via Germany to the Netherlands (Fig. 3a and 3c). This causes a mixing. Downstream, the Rhine River is located in the Cfb region (Fig. 1). In this climate, VT and SSI-6 droughts usually start by the end of summer to early winter (see neighboring rivers). However, our analysis shows that the VT and SSI-6 droughts in the downstream part mostly start before summer. Short drought events in winter/spring in the upstream part of the Rhine play an important role in drought timing in the downstream area (Fig. 3 around Alpine region, ET climate). This also applies when SSI-6 is replaced with SSI-1 (Fig. A2). The FT drought, on the other hands, has drought timing in the end of autumn (Fig. 3b).





Another clear distinction between VT drought timing and climate regions is also found in the Ebro River in Spain. The upstream part of the Ebro River is mainly located in the Cfb climate region where the water is coming from the Pyrenees mountains (Dfc and ET), whereas the downstream part is located in the Bsk climate region. The timing of drought event in the upstream part is early (spring), similar to the Rhine in the upstream part, which mixes the timings of Dfc, ET, and Cfb climates. The downstream part has similar drought timing than many other Cfb and Bsk climate regions, where drought starts at the end of summer to early winter. However, in contrary to VT drought, FT drought, SSI-6, and SSI-1 droughts in the Ebro River do not show different timing between upstream and downstream areas (Fig. 3b,c and A2).

### 3.1.3 Drought occurrences in selected rivers

For a more detailed analysis on differences of streamflow droughts derived from different indices, we investigated four rivers situated in main climates across Europe (Fig. 4 and 5). Figure 4 and 5 show for some particular years a detailed analysis of drought in the rivers. The 30DMA hydrograph of the period 2000-2004 from the Rhine River in combination with the VT and FT clearly shows that streamflow drought mainly occurred from summer to autumn 2003 (Fig. 4a). The year 2003 is one of the most notable drought years in Europe (Fink et al., 2006; Ionita et al., 2017; Laaha et al., 2017). During wet years, e.g. from 2000 to 2002, there were no streamflow drought events (both VT and FT) identified, although the lowest flows occurred in the end of summer season (referred to as the n-day annual minimum flow, which appears each year by definition, Hisdal et al. (2004)). Drought in the Rhine River derived from SSI-6 shows that streamflow drought started in spring 2003 and continued into 2005 (Fig. 5a). This multi-year drought event (Tallaksen and Van Lanen, 2004) occurred because the 6-month accumulated Rhine streamflow was relatively low from 2003 to 2005 (1700-1800 m<sup>3</sup>/s) compared with long mean annual average (>2000 m<sup>3</sup>/s). One long drought event derived from SSI-6 is divided into four shorter SSI-1 drought events (Fig. 5a), which occurred in the beginning of 2003 to December 2003, January 2004 to July 2004, August 2004, and from September 2004 to 2005. A comparison between SSI-6 and SSI-1 droughts clearly shows that the frequency of SSI-1 drought is much higher than of SSI-6 (Vidal et al., 2010) (see also Fig 2c and A1).

In the Danube River (Fig. 4b), FT and VT droughts in 2003 happened in August, whereas in the hydrological year 2004, only FT drought occurred in 2003/2004 winter (November 2003 to January 2004). Similar to the Rhine River, in the Danube, a long SSI-6 drought started before summer of 2003 and covered the whole of 2004 (Fig. 5b). Figures 4b and 5b demonstrate that during rather wet years (year 2000-2002), no VT and SSI-6 droughts were observed. VT and SSI-6 droughts take into account seasonality in their analyses. In contrast, many minor FT drought events were observed if the 30DMA approach would not have been applied to the streamflow data. In these years, several drought events were also seen in SSI-1 (Fig. 5b).

Figure 4c shows that the Kemijoki River, located in the cold climate region (Fig. 1), is dominated by long baseflow periods. High streamflow was only observed at the end of the spring season and summer due to the snowmelt and high precipitation events. Unlike VT drought, which was only identified in the beginning of summer 2004 for short period, a FT drought with long duration and high deficit volume was observed from winter to end of spring 2004 due to delayed snowmelt. A multi-year SSI-1 drought and SSI-6 drought was observed from summer 2002 to the beginning of 2005 (Fig. 5c). During these years, the spring peak streamflow was only half of the peak in the year 2000 and 2001.



285 In the first decade of the 21<sup>st</sup> C, regions situated in the Mediterranean experienced different climate variability compared  
to the rest of Europe. In contrast to the severe 2003 drought in central and west Europe, the most severe droughts in e.g.  
Catalonia (Spain) were observed from 2005 to 2008 (Martin-Ortega et al., 2012; March et al., 2013), which is illustrated by the  
streamflow of the Ebro River that indicates drought events in these years (Fig. 4d and 5d). Nine FT drought events (30DMA)  
were observed from 2005 to 2008, whereas only six VT droughts were observed. These VT and FT drought events from 2005  
290 to 2008 correspond with two and six SSI-6 and SSI-1 drought events, respectively (Fig. 5d). In the hydrologic year 2006, the  
Ebro River experienced one VT drought and three FT droughts when applying the 30DMA and five VT droughts and five FT  
droughts when the 30DMA was not used. This proves that application of the 30DMA results in less minor droughts and that  
the occurrence of FT and SSI-1 droughts in many rivers, not only in the Ebro River, is higher than the VT and SSI-6 droughts,  
as discussed above (Section 3.1.1).

295 In general, our study on streamflow drought occurrences of the four selected rivers and the pan-European river network  
shows that the FT approach identifies more drought events and higher drought deficit volumes than the VT method, which  
contradicts with some previous studies (e.g., Sung and Chung , 2014; Heudorfer and Stahl , 2017). These studies conclude  
that the VT approach yields a higher number of minor drought events and larger deficit volumes because those studies did not  
smooth streamflow and threshold data by applying e.g. 30DMA to reduce the occurrence of minor drought as we did (Section  
300 2b). Another study by Sarailidis et al. (2019) for the Yermasoyia river basin (intermittent river) in Cyprus conclude that FT  
identifies lower number drought event but it yields higher deficit volume than VT, which is in between our study and studies  
conducted by Sung and Chung (2014) and Heudorfer and Stahl (2017).

### 3.1.4 Summary of drought occurrences and timing in selected rivers

The number of streamflow droughts derived using different identification methods and the timing for the four selected rivers  
305 are summarized in Table 1 for the hydrological years 1991 to 2018. We ranked the timing of drought for the two or three  
months, in which drought most frequently occurred starting by the month with the highest occurrence, followed by the month  
with the second highest occurrence, etc (descending order). The highest number of VT drought events was found in the Ebro  
River followed by the Rhine River. The Kemijoki and Danube Rivers have the same number of VT droughts (17 events). The  
frequency of FT droughts is higher than VT droughts (except for the Rhine River). The Ebro River has the highest occurrence  
310 of FT droughts (35 events) followed by the Danube River (32 events). The Kemijoki and Rhine Rivers have a lower number  
of FT drought events than the two other rivers. The occurrence of SSI-6 drought is, in general, close to VT drought around 18  
events, except in Ebro (only 14 SSI-6 drought events).

Another distinction among drought indices is to be seen in the timing of these events, except for Rhine. In the Rhine River  
(downstream, see Fig. 2) streamflow drought mostly occurred in spring for all indices (April), followed by in the beginning  
315 of winter and in autumn. VT and SSI-6 droughts happening in December are caused by sustained low flows in the end of  
summer and autumn. Minor drought events in spring can be related to the warm snow season drought in the upstream area, as  
explained above (Section 3.1.1). In the Danube, VT drought occurred in a wide range of months (spring, end of winter season,  
and summer), while the FT drought commonly occurred at the end of autumn and winter. SSI-6 differs from VT and FT in the



320 Danube. SSI-6 drought mainly occurred in winter and beginning of spring. In the Kemijoki River (Dfc), VT drought has timing  
in late winter and early spring, just before the high streamflow starts (Korhonen and Kuusisto, 2010) (see also Fig. 4c). This is  
typical for rivers in a subarctic climate, where the snowmelt process generates peak streamflow in early summer, that is, May  
or June (Schneider et al., 2013; van Huijgevoort et al., 2014). FT drought, on the other hand, mostly occurred in winter and  
early spring. SSI-6 drought in Kemijoki has a different timing compared to others. Start of drought was mostly observed in late  
spring and in autumn. The Ebro River has VT drought that starts in early spring and autumn. This likely is caused by the lack of  
325 heavy precipitation associated with convective weather events that normally occur in spring and autumn (Barrera-Escoda and  
Llasat, 2015; van Hateren et al., 2019). Moreover, the VT drought that occurred in autumn (November) can also be triggered  
by sustained low flows that started in summer and continued in autumn (from August to October). Drought identification using  
the FT approach in the Ebro River shows that events mostly occurred in the summer (July and August) prior to the SSI-6  
drought.

### 330 3.2 Implication of the identification approaches to forecast streamflow drought

So far this paper has focused on the historical drought analysis using different identification approaches, which creates a base  
for the implications of the findings for streamflow drought forecasting. This section describes in detail an example of the conse-  
quences of using different drought identification approaches to forecast streamflow drought. Figure 6 illustrates the forecasted  
streamflow in the Rhine River (location 1) initiated in August 2003 for 5 months ahead (purple line), incl. 25 ensemble mem-  
335 bers (grey shaded area) and the median ensemble streamflow. In addition, the forecasted droughts in streamflow using different  
identification approaches are given (shaded areas below VT and FT). August 2003 was chosen because streamflow drought  
based on observations (SFO) was starting from this month (see Fig. 4a). Clearly, meteorological drought started earlier. FT  
drought forecast done in August using the median ensemble identifies a drought event that occurred from end of August to mid  
September (Fig. 6a), i.e. the purple line is below the red line. The FT approach forecasts a drought deficit volume of 1,217 m<sup>3</sup>  
340 for the duration of 29 days (red area, Fig. 6a). The VT method, however, could not detect drought and could have performed  
better in this case. The median streamflow is forecasted slightly higher than the VT threshold and consequently no drought  
is predicted. In contrast to the threshold approaches, the 25 ensemble forecasts done in August 2003 using the standardized  
approach (SSI-6) show a long drought event, with SSI-6 that varies between -0.3 and -2.7 (mild to extreme drought) by the  
end of December (Fig. 6b). Based on median ensemble, a mild SSI-6 drought was forecasted for the Rhine at the beginning of  
345 August that increased to severe drought in the end of December.

Figure 6c shows drought forecasts for the Rhine River using VT and FT without applying the smoothing procedure (30DMA).  
Three drought events were forecasted: one in August (both VT and FT indicated by blue and red areas, respectively), one in  
the end of September (FT, red area), and one in the end of October (minor FT drought, red area). FT drought analysis without  
30DMA procedure will produce more drought events with shorter duration (24 days in August, 18 days in September, and  
350 four days in October). The 30DMA FT drought in August 2003 has drought duration of 29 days (see Fig. 6a), which is five  
days longer than without 30DMA application. In total, the FT approach without 30DMA procedure forecasts a drought deficit



volume of 5,047 m<sup>3</sup> in 46 days for the period from August to December 2003. VT drought was only predicted to occur in August with a drought deficit volume of 2,101 m<sup>3</sup> over 18 days.

365 Although VT drought in the example of August 2003 could not be predicted using the 30DMA, a moving average method (e.g. the 30DMA) is commonly applied to reduce minor drought events as shown in some studies (e.g., Fleig et al., 2006; van Loon and Van Lanen, 2012; Sarailidis et al., 2019). For drought forecasting, it is also encouraged to use monthly averaged streamflow data, by for instance, aggregating the data into monthly, such as the use of the Standardized Indices or applying 30DMA (e.g., Yuan and Wood, 2013; Yuan et al., 2013; Dutra et al., 2014; Trambauer et al., 2015; Sutanto et al., 2020a; van Hateren et al., 2019). The use of monthly averaged data or 30DMA will alleviate the drought forecast skill as shown  
360 in those studies. In our case where the 30DMA VT drought could not be detected (Fig. 6a), this might be due to the Q90 threshold applied in our analysis that only identifies rare extreme drought events compared to lower thresholds, such as Q70 and Q80 (Tallaksen et al., 1997; van Loon and Van Lanen, 2012). The SSI-6 also predicts moderate drought in August 2003 ( $-1 > SSI \geq -1.5$ ) and severe drought in October 2003 ( $-1.5 > SSI \geq -2$ ) while no extreme drought was forecasted ( $SSI < -2$ , Fig. 6b).

#### 365 4 Conclusions

Streamflow drought forecasting involves different identification approaches to identify drought. This study presents a historical drought analysis for pan-European rivers, incl. a more detailed investigation of four selected rivers in different climates across Europe using commonly applied identification approaches, which are the Variable Threshold (VT), the Fixed Threshold (FT), and the Standardized Streamflow Index (SSI-6). These approaches generate different drought outcome. The main difference  
370 between VT, FT, and SSI-6 droughts was found in the number of occurrences. The occurrence of drought derived using the FT method is higher than the number of drought events derived using the VT or SSI-6 approach (except SSI-1), which highlights the importance whether end-users of drought forecasts would take seasonality into account or not for their purpose. In addition, the FT method produces higher drought deficit volumes and duration than VT. Identification of streamflow droughts using different methods also affects timing, i.e. the month in which the event starts. Differences are strongly controlled by climate  
375 regions. For instance, in the temperate oceanic climate and Mediterranean climate, FT droughts mostly occurred in the summer (July and August). The start of VT and SSI-6 droughts is later. We also found that, in general, the occurrence and timing of FT droughts are close to what being identified by the SSI-1 index and VT droughts are more similar to SSI-6.

Drought forecasting requires multi-monthly or seasonal time horizons, as drought is a slowly-develop natural disaster that can last longer than a month up to seasons or years. For streamflow drought, the threshold approaches have to be applied  
380 with caution, in particular the temporal aggregation has to be considered. The use of aggregated daily streamflow data into monthly time windows, such as the application of 30-day Moving Average (30DMA), is recommended as applied in this study for the identification of VT and FT droughts. This approach will eliminate the undesired minor drought events, which are identified when using non-aggregated daily flow data, and also increase the drought forecast skill. The use of monthly-aggregated forecasted flow data (e.g. SSI) is the best practice for seasonal drought forecasts. This method, however, cannot be



385 used to calculate the drought deficit volume, which is a key component for water managers coping with hydrological drought. If  
deficit volumes are required for decision making, then threshold approaches (VT or FT) should be applied on 30-day averaged  
flow data. The choice of the drought identification method when forecasting streamflow drought, in the end, lies to the end-users  
specific requirements and decisions and there is no one drought identification approach that fits all needs.

Our study clearly shows that streamflow droughts obtained from different drought identification approaches (variable thresh-  
old, fixed threshold, and standardized approaches) differ both in the occurrence and timing, including the forecasts of these  
390 events. Often scientists have analyzed and provided streamflow drought forecasts without clearly defining the identification  
method. This created misconceptions, miss-citations, and confusion among the academic community (authors, reviewers, ed-  
itors), operational weather and water services, as well as end-users, which consider drought forecast products and associated  
terminology as interchangeably. Our study recommends scientists, developers of Drought Early Warning Systems and end-  
395 users to clearly agree among themselves upon a sharp definition which type of streamflow drought is required to be forecasted  
to mitigate the impacts of drought. Obviously, Drought Early Warning Systems also can include more than one drought iden-  
tification method, as illustrated by Sutanto et al. (2020a). Then the end-user can decide in the end which forecast product is  
most adequate based upon the provided description of the identification method and product.

*Data availability.* The streamflow EFAS data are accessible under a COPERNICUS open data license (<https://doi.org/10.24381/cds.e3458969>).  
400 In this study, we used EFAS system version 3. The SSI-6 and SSI-1 analyzed using the SFO data and re-forecasts are available online in the  
4TU Centre for Research Data with doi:xxxxx.

## Appendix A: Drought occurrence and timing derived from SSI-1

In Figure A1, we present the number of streamflow drought occurrences identified using the Standardized Streamflow Index  
with an accumulation time of one month (SSI-1). Streamflow drought was calculated using the SFO data from 1990 to 2018.  
405 Occurrence of streamflow drought derived from SSI-1 is higher than SSI-6 (Fig. 2c), which is more than 70 events in some  
regions, such as in the UK and Norway. Figure S2 shows the timing of streamflow drought identified using the SSI-1. Major  
difference between SSI-1 and SSI-6 (Fig. 3c) in term of drought timing is located in the Dfb (central and east Europe) and Dfc  
climate regions (north Europe). In these regions the timing of SSI-1 is in winter and spring, which deviates with the timing of  
SSI-6 in autumn.

410 *Author contributions.* S.J.S and H.A.J.V.L conceived and implemented the research. Data analyses, model output analyses, and all figures  
have been performed by S.J.S. S.J.S and H.A.J.V.L wrote the initial version of the paper and equally contributed to interpreting the results,  
discussion, and improving the paper.



*Competing interests.* The authors declare no competing financial and/or non-financial interests in relation to the work described.

*Acknowledgements.* The research is supported by the ANYWHERE project (Grant Agreement No.: 700099), which is funded within EU's  
415 Horizon 2020 research and innovation program ([www.anywhere-h2020.eu](http://www.anywhere-h2020.eu)). The streamflow data came from the EFAS computational center, which is part of the Copernicus Emergency Management Service (EMS) and Early Warning Systems (EWS) funded by framework contract number 198702 of the European Commission. We thank Fredrik Wetterhall (ECMWF) for providing the EFAS data. This research is part of the Wageningen Institute for Environment and Climate Research (WIMEK-SENSE) and it supports the work of UNESCO EURO FRIEND-Water and the IAHS Panta Rhei program of Drought in the Anthropocene.



## 420 References

- Arnal, L., Asp, S.-S., Baugh, C., De Roo, A., Disperati, J., Dottori, F., Garcia, R., Garcia-Padilla, M., Gelati, E., Gomes, G., Kalas, M., Krzeminski, B., Latini, M., Lorini, V., Mazzetti, C., Mikulichova, M., Muraro, D., Prudhomme, C., Rauthe-Schoch, A., Rehfeldt, K., Salamon, P., Schweim, C., Skoien, J.O., Smith, P., Sprokkereef, E., Thiemiig, V., Wetterhall, F., and Ziese, M.: EFAS upgrade for the extended model domain-technical documentation. Publications Office of the European Union, Luxembourg, EUR 29323 EN (ISBN 978-92-79-92881-9), <https://doi.org/10.2760/806324>, 2019.
- 425 Arnal, L., Cloke, H. L., Stephens, E., Wetterhall, F., Prudhomme, C., Neumann, J., Krzeminski, B., and Pappenberger, F.: Skilful seasonal forecasts of streamflow over Europe?, *Hydrol. Earth Syst. Sci.*, 22, 2057–2072, <https://doi.org/10.5194/hess-22-2057-2018>, 2018.
- Barker, L. J., Hannaford, J., Chiveron, A., and Svensson, C.: From meteorological to hydrological drought using standardised indicators, *Hydrol. Earth Syst. Sci.*, 20, 2483–2505, doi:10.5194/hess-20-2483-2016, 2016.
- 430 Barrera-Escoda, A., and Llasat, M. C.: Evolving flood patterns in a Mediterranean region (1301–2012) and climatic factors—the case of Catalonia, *Hydrol. Earth Syst. Sci.*, 19, 465–483, doi:10.5194/hess-19-465-2015, 2015.
- Bell, V. A., Davies, H. N., Kay, A. L., Brookshaw, A., and Scaife, A. A.: A national-scale seasonal hydrological forecast system: development and evaluation over Britain, *Hydrol. Earth Syst. Sci.*, 21, 4681–4691, 2017.
- Belayneh, A., Adamowski, J., Khalil, B., and Ozga-Zielinski, B.: Long-term SPI drought forecasting in the Awash River Basin in Ethiopia using wavelet neural network and wavelet support vector regression models, *Journal of Hydrology*, 508: 418–429, <https://doi.org/10.1016/j.jhydrol.2013.10.052>, 2014.
- 435 Burek, P., van der Knijff, J., and Roo, A. D.: LISFLOOD distributed water balance and flood simulation model, JRC Tech. Report, <https://doi.org/10.2788/24719>, 2013a.
- Burek, P., van der Knijff, J., and Ntegeka, V.: LISVAP Evaporation Pre-processor for the LISFLOOD water balance and flood simulation model, JRC Tech. Rep., EUR26167EN, doi:10.2788/26000, 2013b.
- 440 Changnon, S. A.: Detecting drought conditions in Illinois, Champaign Circular 169, Illinois State Water Survey, 36 pp., [ISWS/CIR-169/87], 1987.
- Clark, M. P., and Hay, L. E.: use of medium-range numerical weather prediction model output to produce forecasts of streamflow, *Journal of Hydrometeorology*, 5, 15–32, 2004.
- 445 Cloke, H., Pappenberger, F., Thielen, J., and Thiemiig, V.: Operational European flood forecasting, in: *Environmental Modelling: Finding Simplicity in Complexity*, 2nd edn., Wainwright, J. and Mulligan, M. (Eds.). John Wiley and Sons, Ltd, Chichester, UK, <https://doi.org/10.1002/9781118351475.ch25>, 2013.
- Day, G. N.: Extended Streamflow Forecasting Using NWSRFS, *Journal of Water Resources Planning and Management*, 111(2), 157–170, 1985.
- 450 Ding, Y., Hayes, M., and Widhalm, M.: Measuring economic impacts of drought: a review and discussion, *Disaster Prevention and Management*, Vol. 20 No. 4, pp. 434–446, <https://doi.org/10.1108/09653561111161752>, 2011.
- Duan, Q., Pappenberger, F., Wood, A., Cloke, H. L., and Schaake, J. C.: *Handbook of Hydrometeorological Ensemble Forecasting*, Springer, <https://doi.org/10.1007/978-3-642-39925-1>, 2019.
- Dutra, E., Pozzi, W., Wetterhall, F., Di Giuseppe, F., Magnusson, L., Naumann, G., Barbosa, P., Vogt, J., and Pappenberger, F.: Global meteorological drought – Part 2: Seasonal forecasts, *Hydrol. Earth Syst. Sci.*, 18, 2669–2678, doi:10.5194/hess-18-2669-2014, 2014.
- 455



- Feyen, L., and Dankers, R.: Impact of global warming on streamflow drought in Europe, *J. Geophys. Res.*, 114, D17116, doi:10.1029/2008JD011438, 2009.
- Fink, A. H., Brücher, T., Krüger, A., Leckebusch, G. C., Pinto, J. G., and Ulbrich, U.: The 2003 european summer heatwaves and drought-synoptic diagnosis and impacts, *Weather, Royal Meteor. Soc.*, 59, 209–216, doi:10.1256/wea.73.04, 2006.
- 460 Fleig, A. K., Tallaksen, L. M., Hisdal, H., and Demuth, S.: A global evaluation of streamflow drought characteristics, *Hydrol. Earth Syst. Sci.*, 10, 535–552, 2006.
- Forzieri, G., Feyen, L., Rojas, R., Flörke, M., Wimmer, F., and Bianchi, A.: Ensemble projections of future streamflow droughts in Europe, *Hydrol. Earth Syst. Sci.*, 18, 85–108, doi: 10.5194/hess-18-85-2014, 2014.
- Fundel, F., Jörg-Hess, S., and Zappa, M.: Monthly hydrometeorological ensemble prediction of streamflow droughts and corresponding  
465 drought indices, *Hydrol. Earth Syst. Sci.*, 17, 395–407, doi:10.5194/hess-17-395-2013, 2013.
- Gu, L., Chen, J., Yin, J., Sullivan, S. C., Wang, H-M., Guo, S., Zhang, L., and Kim, J-S.: Projected increases in magnitude and socioeconomic exposure of global droughts in 1.5 and 2°C warmer climates, *Hydrol. Earth Syst. Sci.*, 24, 451–472, <https://doi.org/10.5194/hess-24-451-2020>, 2020.
- Haile, G. G., Tang, Q., Sun, S., Huang, Z., Zhang, X., and Liu, X.: Droughts in East Africa: Causes, impacts and resilience, *Earth-Science  
470 Reviews*, 193, 146–161, <https://doi.org/10.1016/j.earscirev.2019.04.015>, 2019.
- Hannaford, J., Lloyd-Hughes, B., Keef, C., Parry, S., and Prudhomme, C.: Examining the large-scale spatial coherence of European drought using regional indicators of precipitation and streamflow deficit, *Hydrol. Process.*, 25, 1146–1162, doi:10.1002/hyp.7725, 2011.
- Heudorfer, B., and Stahl, K.: Comparison of different threshold level methods for drought propagation analysis in Germany, *Hydrology Research*, 48.5, 1311–1326, doi:10.2166/nh.2016.258, 2017.
- 475 Hisdal, H., Tallaksen, L. M., Clausen, B., Peters, E., and Gustard, A.: Hydrological Drought Characteristics. In: Tallaksen, L. M. & Van Lanen, H. A. J. (Eds.) *Hydrological Drought, Processes and Estimation Methods for Streamflow and Groundwater. Development in Water Science 48*, Elsevier Science B.V., pg. 139–198, 2004.
- Ionita, M., Tallaksen, L. M., Kingston, D> G., Stagge, J. H., Laaha, G., Van Lanen, H. A. J., Scholz, P., Chelcea, S. M., and Haslinger, K.:  
480 The european 2015 drought from a climatological perspective, *Hydrol. Earth Syst. Sci.*, 21, 1397–1419, doi:10.5194/hess-21-1397-2017, 2017.
- IPCC.: *Climate Change 2014: Synthesis Report. Contribution of Working Groups I, II and III to the Fifth Assessment Report of the Intergovernmental Panel on Climate Change [Core Writing Team, R.K. Pachauri and L.A. Meyer (eds.)]*. IPCC, Geneva, Switzerland, 151 pp, 2014.
- Jakubowski, W., and Radczuk, L.: Estimation of Hydrological Drought Characteristics, NIZOWKA2003 – Software Manual, on accompanying CD to: *Hydrological Drought – Processes and Estimation Methods for Streamflow and Groundwater*, edited by: Tallaksen, L. M. and van Lanen, H. A. J., *Developments in Water Science*, 48, Elsevier Science B.V., Amsterdam, 2004.
- Korhonen, J., and Kuusisto, E.: long-term changes in the discharge regime in Finland, *Hydrology Research*, 41.3–4, 253–268, doi:10.2166/nh.2010.112, 2010.
- Laaha, G., Gauster, T., Tallaksen, L. M., Vidal, J-P., Stahl, K., Prudhomme, C., Heudorfer, B., Vlnas, R., Ionita, M., Van Lanen, H. A. J.,  
490 Adler, M-J., Cailouet, L., Delus, C., Fendekova, M., Gailliez, S., Hannaford, J., Kingston, D., Van Loon, A. F., Mediero, L., Ozuch, M., Romanowicz, R., Sauquet, E., Stagge, J. H., and Wong, W. K.: The european 2015 drought from a hydrological perspective, *Hydrol. Earth Syst. Sci.*, 21, 3001–3024, doi:10.5194/hess-21-3001-2017, 2017.





- March, H., Domènech, L., and Saurí, D.: Water conservation campaigns and citizen perceptions: the drought of 2007-2008 in the Metropolitan area of Barcelona, *Nat. Hazards*, 65, 1951-1966, doi:10.1007/s11069-012-0456-2, 2013.
- 495 Martin-Ortega, J., González-Eguino, M., and Markandya, A.: The costs of drought: the 2007/2008 case of Barcelona, *Water Policy*, 14, 539-560, doi:10.2166/wp.2011.121, 2012.
- Marx, A., Kumar, R., Thober, S., Rakovec, O., Wanders, N., Zink, M., Wood, E. F., Pan, M., Sheffield, J., and Samaniego, L.: Climate change alters low flows in Europe under global warming of 1.5, 2, and 3°C, *Hydrol. Earth Syst. Sci.*, 22, 1017-1032, doi:10.5194/hess-22-1017-2018, 2018.
- 500 McKee, T. B., Doesken, N. J., and Kleist, J.: The relationship of drought frequency and duration to time scales. In: *Proceedings of the 8<sup>th</sup> Conference on Applied Climatology*, Vol. 17, American Meteorological Society Boston, MA, pp. 179-183, 1993.
- Mendoza, P. A., Wood, A. W., Clark, E., Rothwell, E., Clark, M. P., Nijssen, B., Brekke, L. D., and Arnold, J. R.: An intercomparison of approaches for improving operational seasonal streamflow forecasts, *Hydrol. Earth Syst. Sci.*, 21, 3915-3935, doi:10.5194/hess-21-3915-2017, 2017.
- 505 Mishra, A. K., and Singh, V. P.: A review of drought concepts, *Journal of Hydrology*, 391, 202-216, <https://doi.org/10.1016/j.jhydrol.2010.07.012>, 2010.
- Mishra, A.K., and Desai, V.R.: Drought forecasting using stochastic models, *Stoch. Environ. Res. Ris. Assess.*, 19, 326-339, <https://doi.org/10.1007/s00477-005-0238-4>, 2005.
- Nalbantis, I., and Tsakiris, G.: Assessment of hydrological drought revisited, *Water Resour. Manage.*, 23, 881-897, doi:10.1007/s11269-008-510 9305-1, 2009.
- Pappenberger, F., Thielen, J., and Del Medico, M.: The impact of weather forecast improvements on large scale hydrology: analyzing a decade of forecasts of the European Flood Alert System, *Hydrol. Process.*, 25, 1091-1113, <https://doi.org/10.1002/hyp.7772>, 2011.
- Peel, M. C., Finlayson, B. L., and McMahon, T. A.: Updated world map of the Köppen-Geiger climate classification, *Hydrol. Earth Syst. Sci.*, 11, 1633-1644, 2007.
- 515 Peters, E., Bier, G., Van Lanen, H. A. J., and Torfs, P. J. J. F.: Propagation and spatial distribution of drought in a groundwater catchment, *J. Hydrol.*, 321, 257-275, doi:10.1016/j.jhydrol.2005.08.004, 2006.
- Peters, E. P., Torfs, J. J. F., Van Lanen, H. A. J., and Bier, G.: Propagation of drought through groundwater-a new approach using linear reservoir theory, *Hydrol. Process.*, 17, 3023-3040, 2003.
- Pfister, C., Weingartner, R., and Luterbacher, J.: Hydrological winter droughts over the last 450 years in the upper Rhine basin: a method-  
520 ological approach, *Hydrological Sciences Journal*, 51:5, 966-985, doi:10.1623/hysj.51.5.966, 2006.
- Poljanšek, K., Marin Ferrer, M., De Groeve, T., and Clark, I.: Science for disaster risk management 2017: knowing better and losing less, executive summary, EUR 28034 EN, ISBN 978-92-79-60679-3, <https://doi.org/10.2788/842809>, JRC102482, 2017.
- Pozzi, W., Sheffield, J., Stefanski, R., Cripe, D., Pulwarty, R., Vogt, J. V., Heim Jr, R. R., Brewer, M. J., Svoboda, M., Westerhoff, R., . . . . . ,  
525 and Lawford, R.: Toward global drought early warning capability: Expanding international cooperation for the development of a framework for monitoring and forecasting, *Bulletin of the American Meteorological Society*, 94 (6), 776-785, <https://doi.org/10.1175/BAMS-D-11-00176.1>, 2013.
- Prudhomme, C., Giuntoli, I., Robinson, E. L., Clark, D. B., Arnell, N. W., Dankers, R., Fekete, B. M., Fransses, W., Gerten, D., Gosling, S. N., Hagemann, S., Hannah, D. M., Kim, H., Masaki, Y., Satoh, Y., Stacke, T., Wada, Y., and Wisser, D.: Hydrological droughts in the 21<sup>st</sup> century, hotspots and uncertainties from a global multimodel ensemble experiment, *PNAS*, vol.111, no.9, 3262-3267,  
530 doi:10.1073/pnas.1222473110, 2014.



- Prudhomme, C., Parry, S., Hannaford, J., Clark, D. B., Hageman, S., and Voss, F.: How well do large-scale models reproduce regional hydrological extremes in Europe? *Journal of Hydrometeorology*, 12, 1181–1204, doi:10.1175/2011JHM1387.1, 2011.
- Samaniego, L., Thober, S., Kumar, R., Wanders, N., Rakovec, O., Pan, M., Zink, M., Sheffield, J., Wood, E. F., and Marx, A.: Anthropogenic warming exacerbates European soil moisture droughts, *Nature Climate Change*, 8, 421–426, doi:10.1038/s41558-018-0138-5, 2018.
- 535 Sarailidis, G., Vasiliades, L., and Loukas, A.: Analysis of streamflow droughts using fixed and variable thresholds, *Hydrological Processes*, 33, 414–431, <https://doi.org/10.1002/hyp.13336>, 2019.
- Schaake, J. C., Hamill, T. M., Buizza, R., and Clark, M.: HEPEX: the hydrological ensemble prediction experiment, *Bulletin of the American Meteorological Society*, 88(10), 1541–1547, 2007.
- Schneider, C., Laize, C. L. R., Acreman, M. C., and Flörke, M.: How will climate change modify river flow regimes in Europe? *Hydrol. Earth Syst. Sci.*, 17, 325–339, doi:10.5194/hess-17-325-2013, 2013.
- 540 Sivakumar, M. V. K., Stefanski, R., Bazza, M., Zelaya, S., Wilhite, D., and Magalhaes, A. R.: High Level Meeting on National Drought Policy: Summary and Major Outcomes, *Weather and Climate Extremes*, 3, 126–132, <http://dx.doi.org/10.1016/j.wace.2014.03.007>, 2014.
- Slater, L. J., and Villarini, G.: Enhancing the predictability of seasonal streamflow with a statistical-dynamical approach, *Geophysical Research Letters*, 45(13), pp.6504–6513, 2018.
- 545 Stahl, K., Kohn, I., Blauhut, V., Urquijo, J., De Stefano, L., Aca´cio, V., Dias, S., Stagge, J. H., Tallaksen, L. M., Kampragou, E., . . . , and Van Lanen, H. A. J.: Impacts of european drought events: insights from an international database of text-based reports., *Natural Hazards and Earth System Sciences*, 16 (3), 801–819, <https://doi.org/10.5194/nhess-16-801-2016>, 2016.
- Stockdale, T., Johnson, S., Ferranti, L., Balmaseda, M., and Briceag, S.: ECMWF’s new long range forecasting system SEAS5, Vol. 154. *ECMWF Newsletter*, doi:10.21957/tsb6n1, 2018.
- 550 Sung, J. H., and Chung, E.-S.: Development of streamflow drought severity-duration-frequency curves using the threshold level method, *Hydrol. Earth Syst. Sci.*, 18, 3341–3351, doi:10.5194/hess-18-3341-2014, 2014.
- Sutanto, S. J., Van Lanen, H. A. J., Wetterhall, F., and Lloret, X.: Potential of pan-European seasonal hydro-meteorological drought forecasts obtained from a Multi-Hazard Early Warning System, *Bulletin of the American Meteorological Society*, 101, 368–393, <https://doi.org/10.1175/BAMS-D-18-0196.1>, 2020a.
- 555 Sutanto, S. J., Wetterhall, F., and Van Lanen, H. A. J.: Hydrological drought forecasts outperform meteorological drought forecasts, *Environ. Res. Lett.*, 15, 084010, <https://doi.org/10.1088/1748-9326/ab8b13>, 2020b.
- Sutanto, S. J., Van der Weert, M., Wanders, N., Blauhut, V., and Van Lanen, H. A. J.: Moving from drought hazard to impact forecasts, *Nat. Comm.*, 10:495, <https://doi.org/10.1038/s41467-019-12840-z>, 2019.
- Tallaksen, L. M., and Van Lanen, H. A. J.: Hydrological drought: processes and estimation methods for streamflow and groundwater, In: *Developments in Water Science*, vol. 48, Amsterdam, the Netherlands: Elsevier Science B.V, 2004.
- 560 Tallaksen, L. M., Madsen, H., and Clausen, B.: On the definition and modeling of streamflow drought duration and deficit volume, *Hydrological Sciences Journal*, 42:1, 15–33, doi:10.1080/02626669709492003, 1997.
- Thielen, J., Bartholmes, J., Ramos, M.-H., and Roo, A. D.: The European Flood Alert System - part 1: concept and development, *Hydrol. Earth Syst. Sci.*, 13, 125–140, <https://doi.org/10.5194/hess-13-125-2009>, 2009.
- 565 Trambauer, P., Werner, M., Winsemius, H. C., Maskey, S., Dutra, E., and Uhlenbrook, S.: Hydrological drought forecasting and skill assessment for the Limpopo River basin, southern Africa, *Hydrology and Earth System Sciences*, 19(4), 1695–1711, 2015.
- Trambauer, P., Maskey, S., Winsemius, H., Werner, M., and Uhlenbrook, S.: A review of continental scale hydrological models and their suitability for drought forecasting in (sub-Saharan) Africa, *Physics and Chemistry of the Earth*, 66, 16–26, 2013.



- 570 Van Der Knijff, J. M., Younis, J., and De Roo, A. P. J.: Lisflood: a gis-based distributed model for river basin scale water balance and flood simulation, *International Journal of Geographical Information Science*, 24:2, 189–212, <https://doi.org/10.1080/13658810802549154>, 2010.
- Van Der Knijff, J.: LISVAP: Evaporation Pre-Processor for the LISFLOOD Water Balance and Flood Simulation Model, EUR 22639 EN/2, 2008.
- 575 Van Dijk, A. I. J. M., Beck, H. E., Crosbie, R. S., de Jeu, R. A. M., Liu, Y. Y., Podger, G. M., Timbal, B., and Viney, N. R.: The Millennium Drought in southeast Australia (2001–2009): Natural and human causes and implications for water resources, ecosystems, economy, and society, *Water Resources Research*, 49, 1040–1057, doi:10.1002/wrcr.20123, 2013.
- Van Hateren, T., Sutanto, S. J., and Van Lanen, H. A. J.: Evaluating uncertainty and robustness of seasonal meteorological and hydrological drought forecasts at the catchment scale-case Catalonia (spain), *Env. Int.*, 133, 105206, <https://doi.org/10.1016/j.envint.2019.105206>, 2019.
- 580 Van Huijgevoort, M. H. J., Van Lanen, H. A. J., Teuling, A. J., and Uijlenhoet, R.: Identification of changes in hydrological drought characteristics from a multi-GCM driven ensemble constrained by observed discharge, *Journal of Hydrology*, 512, 421-434, doi:10.1016/j.hydrol.2014.02.060, 2014.
- Van Lanen, H. A. J., Fendeková, M., Kupczyk, E., Kasprzyk, A., and Pokojski, W.: Flow Generating Processes, in: *Hydrological Drought, Processes and Estimation Methods for Streamflow and Groundwater*, edited by: Tallaksen, L. M. and Van Lanen, H. A. J., Development in Water Science 48, Elsevier Science B.V., 53–96, 2004.
- 585 Van Loon, A. F.: Hydrological drought explained, *WIREs Water*, <https://doi.org/10.1002/wat2.1085>, 2015.
- Van Loon, A. F., and Van Lanen, H. A. J.: A process-based typology of hydrological drought, *Hydrol. Earth Syst. Sci.*, 16, 1915-1946, 2012.
- Van Loon, A. F., Van Huijgevoort, M. H. J., and Van Lanen, H. A. J.: Evaluation of drought propagation in an ensemble mean of large-scale hydrological models, *Hydrol. Earth Syst. Sci.*, 16, 4057-4078, doi:10.5194/hess-16-4057-2012, 2012.
- 590 Van Loon, A. F., Fendeková, M., Hisdal, H., Horvát, O., Van Lanen, H. A. J., Machlica, A., Oosterwijk, J., and Tallaksen, L. M.: Understanding hydrological winter drought in Europe, in: 6th World FRIEND Conference “Global Change: Facing Risks and Threats to Water Resources”, edited by: Servat, E., Demuth, S., Dezetter, A., Daniell, T., Ferrari, E., Ijjaali, M., Jabrane, R., Van Lanen, H. A. J., and Huang, Y., IAHS-AISH P., 340, 189–197, 2010.
- Vicente-Serrano, S. M., López-Moreno, J. I., Beguería, S., Lorenzo-Lacruz, J., Azorin-Molina, C., and Morán-Tejeda, E.: Accurate computation of a streamflow drought index, *J. Hydrol. Eng.*, 17(2), 318-332, doi:10.1061/(ASCE)HE.1943-5584.0000433, 2012.
- 595 Vicente-Serrano, S. M., Begueria, S., and López-Moreno, J. I.: A multi-scalar drought index sensitive to global warming: the standardized precipitation evapotranspiration index-SPEI, *Journal of Climate*, 23(7), 1696–1718, <https://doi.org/10.1175/2009JCLI2909.1>, 2010.
- Vidal, J.-P., Martin, E., Franchistéguy, L., Habets, F., Soubeyroux, J.-M., Blanchard, M., and Baillon, M.: Multilevel and multiscale drought reanalysis over France with the Safran-Isba-Modcou hydrometeorological suite, *Hydrol. Earth Syst. Sci.*, 14, 459–478, <https://doi.org/10.5194/hess-14-459-2010>, 2010.
- 600 Wanders, N., Wada, Y., and Van Lanen, H. A. J.: Global hydrological droughts in the 21<sup>st</sup> century under a changing hydrological regime, *Earth Syst. Dynam.*, 6, 1-15, 2015.
- Wanders, N., Thober, S., Kumar, R., Pan, M., Sheffield, J., Samaniego, L., and Wood, E.: Development and evaluation of a Pan-European multi-model seasonal hydrological forecasting system, *Journal of Hydrometeorology*, 20, 99-115, 2019.
- 605 Wilhite, D. A., Svoboda, M. D., and Hayes, M. J.: Understanding the complex impacts of drought: A key to enhancing drought mitigation and preparedness, *Water Resour. Manage.*, 21, 763–774, doi:10.1007/s11269-006-9076-5, 2007.



- WMO & GWP.: National Drought Management Policy Guidelines: A Template for Action (D. A. Wilhite). Integrated Drought Management Programme (IDMP) Tools and Guidelines Series 1. WMO, Geneva, Switzerland and GWP, Stockholm, Sweden, [https://public.wmo.int/en/resources/library/national-drought-management-policy-guidelines-template-action], 2014.
- 610 Wong, W. K., Beldring, S., Engen-Skaugen, T., Haddeland, I., and Hisdal, H.: Climate Change Effects on Spatiotemporal Patterns of Hydro-climatological Summer Droughts in Norway, *J. Hydrometeorol.*, 12, 1205–1220, doi:10.1175/2011JHM1357.1, 2011.
- Yevjevich, V.: An objective approach to definition and investigations of continental hydrologic droughts, *Hydrology Papers*, 23, Colorado State University, Fort Collins, USA, 1967.
- Yuan X., Zhang, M., Wang, L., and Zhou, T.: Understanding and seasonal forecasting of hydrological drought in the Anthropocene, *Hydrol. Earth Syst. Sci.*, 21, 5477–5492, doi:10.5194/hess-21-5477-2017, 2017.
- 615 Yuan, X., and Wood, E. F.: Multimodel seasonal forecasting of global drought onset, *Geophysical Research Letters*, 40, 4900-4905, doi:10.1002/grl.50949, 2013.
- Yuan, X., Wood, E. F., Chaney, N. W., Sheffield, J., Kam, J., Liang, M., and Guan K.: probabilistic seasonal forecasting of African drought by dynamical models, *Journal of Hydrometeorology*, 14, 1706-1720, doi:10.1175/JHM-D-13-054.1, 2013.

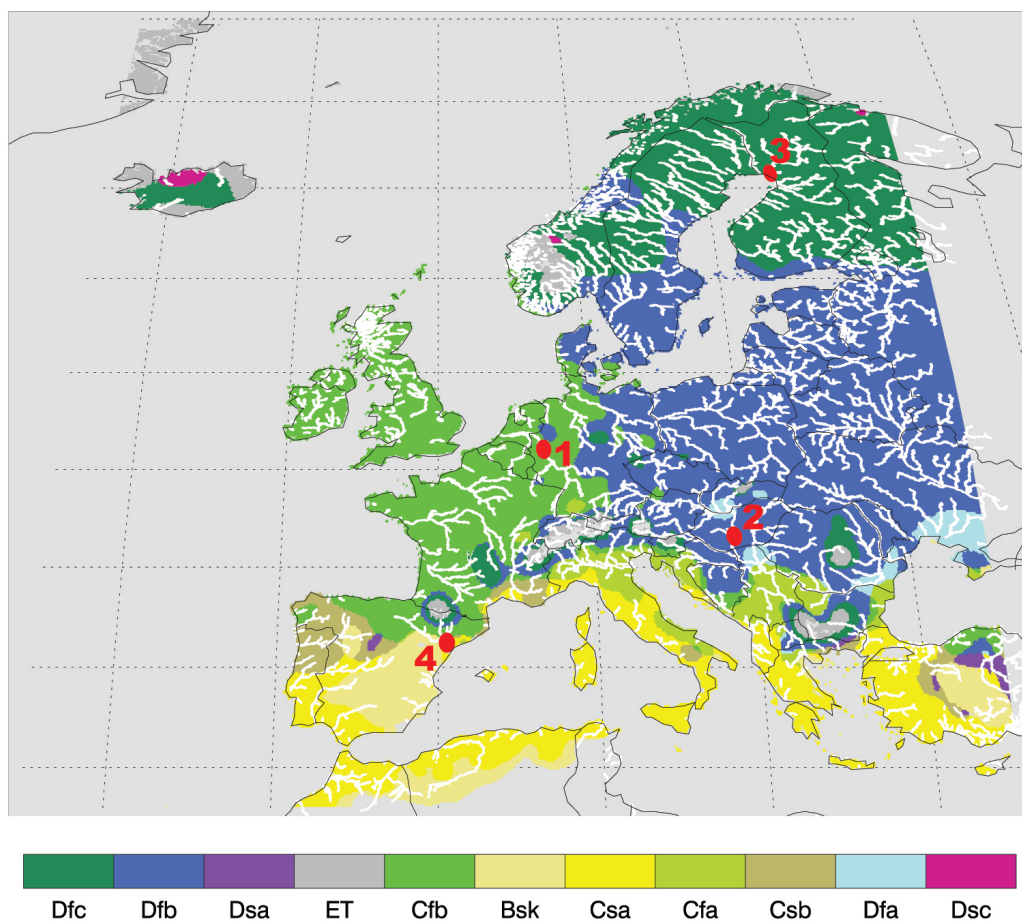


**Figure 1.** Köppen-Geiger map of Europe, and locations of selected river basins for detailed hydrological drought analyses in different climate regimes, as shown by red dots. Readers are referred to Peel et al. (2007) for an explanation of Köppen-Geiger climate classification codes (e.g., Dfc, Dfb, Dsa, and so on).

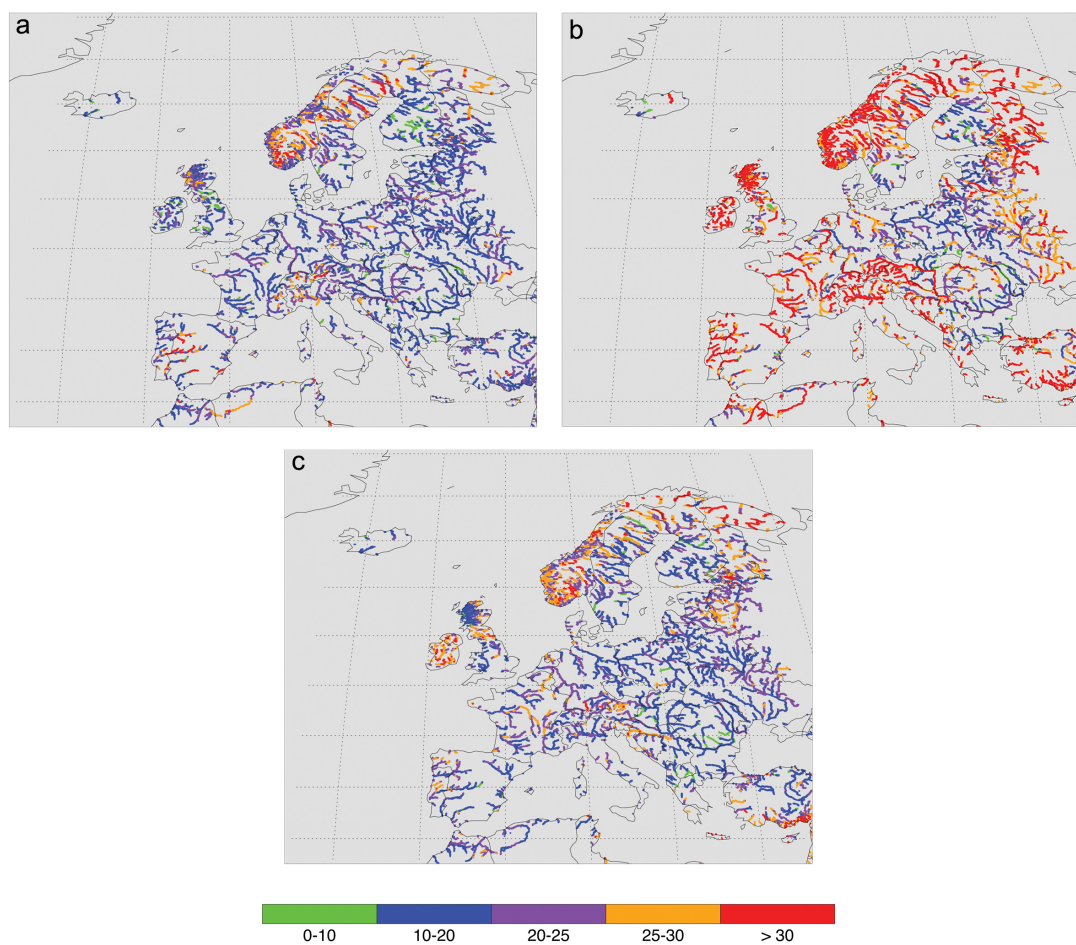


**Figure 2.** a) Drought occurrences in European rivers from October 1990 to September 2018 (28 years) identified using the variable threshold method (VT drought), b) using the fixed threshold method (FT drought), and c) using the Standardized Streamflow Index with accumulation time 6 months (SSI-6 drought).

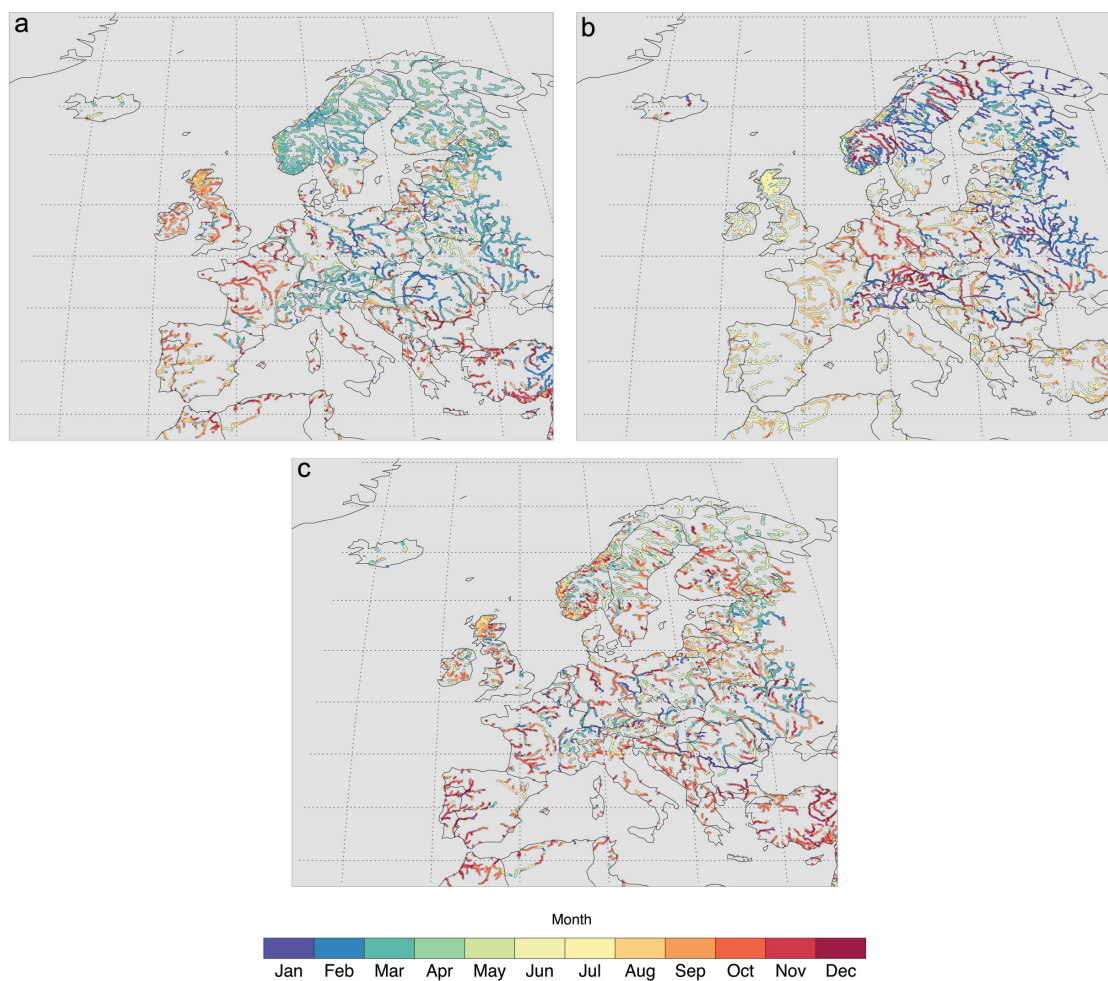


**Figure 3.** a) Months when drought mostly started in the European rivers from October 1990 to September 2018 identified using the variable threshold method (VT drought), b) using the fixed threshold method (FT drought), and c) using the Standardized Streamflow Index with accumulation time 6 months (SSI-6 drought). The timing for drought was determined based on the first month of each drought event.

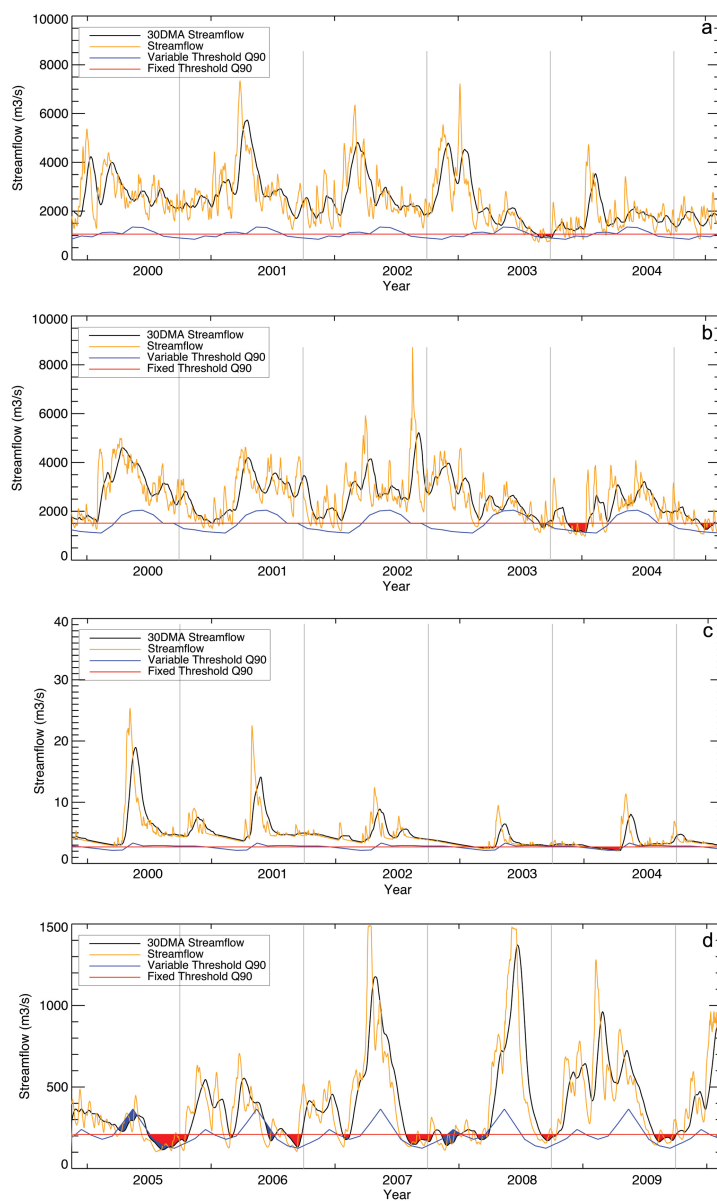


**Figure 4.** Streamflow droughts in the: a) Rhine River from 2000 to 2004 (location 1), b) Danube River from 2000 to 2004 (location 2), c) Kemijoki River from 2000 to 2004 (location 3), and d) Ebro River from 2005 to 2009 (location 4). Streamflow drought events are indicated as blue areas below the threshold for variable threshold (VT drought) and red areas for fixed threshold (FT drought).



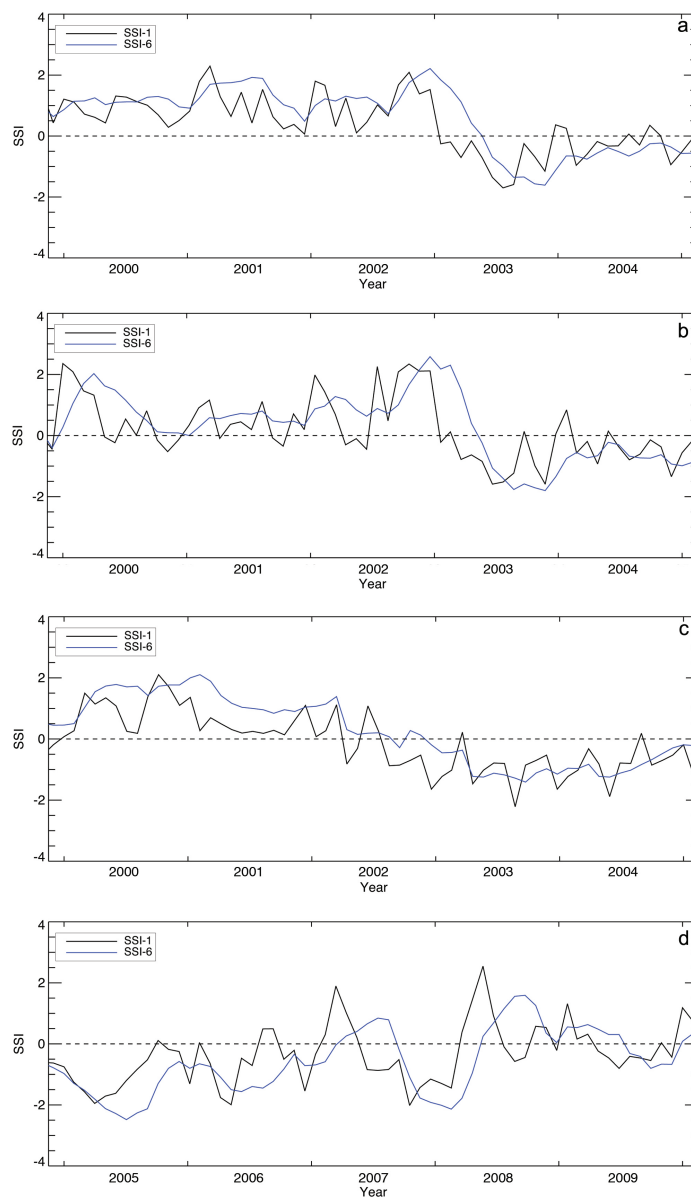


**Figure 5.** Streamflow droughts (SSI-6 and SSI-1 droughts) in the: a) Rhine River from 2000 to 2004 (location 1), b) Danube River from 2000 to 2004 (location 2), c) Kemijoki River from 2000 to 2004 (location 3), and d) Ebro River from 2005 to 2009 (location 4), derived from the Standardized Streamflow Index (SSI) with accumulation periods of 1 and 6-month.

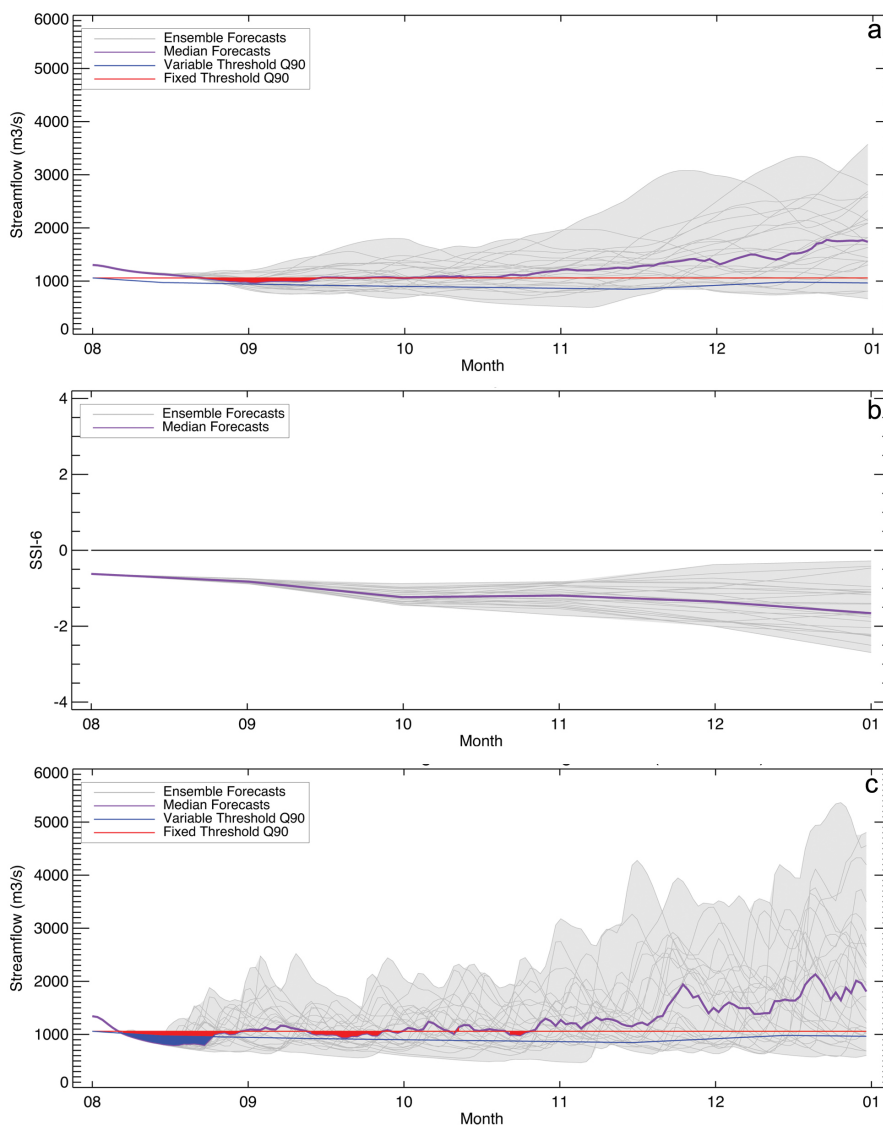


**Figure 6.** Forecasted streamflow for 25 ensemble members and streamflow drought in the Rhine River initiated on 1st August 2003 for 5 months ahead (153 days, gray lines). a) Drought is indicated by the forecasted streamflow (30DMA) below the variable threshold (VT, blue line and blue shaded area) and the fixed threshold (FT, red line and red shaded area), b) SSI-6 drought (persistent drought in the forecast period,  $SSI-6 < 0$ ), and c) same as a) but without 30DMA application to the forecasted streamflow.



**Table 1.** The number of streamflow droughts and timing using the fixed (FT), variable threshold (VT), and SSI-6 approaches for the selected locations in the four rivers (Fig. 1) from hydrologic years 1991 to 2018. The timing for streamflow drought events was determined as the first month when drought occurred. In some results, we only show two months for the timing because the third highest occurrences of timing are too low and close/similar to the fourth and the fifth

No	River	VT drought		FT drought		SSI-6 drought	
		Num. of events	Timing	Num. of events	Timing	Num. of events	Timing
1	Rhine	21	4, 12, 8	19	10, 4, 11	20	4, 12
2	Danube	17	4, 2, 8	32	11, 2, 12	18	3, 1
3	Kemijoki	17	4, 3, 5	21	1, 2, 3	15	10, 5, 6
4	Ebro	24	2, 11, 3	35	8, 2, 7	14	6, 8, 1

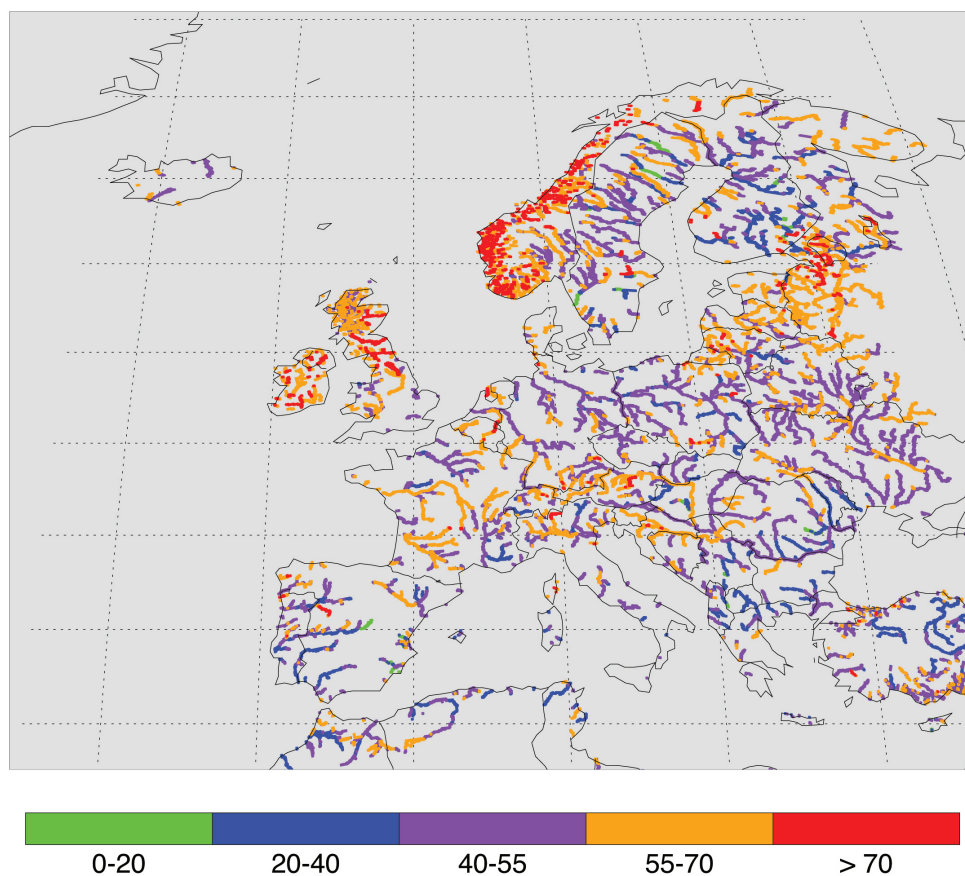


**Figure A1.** Drought occurrences in European rivers from October 1990 to September 2018 (28 years) identified using the Standardized Streamflow Index with accumulation time of 1-month (SSI-1). One should note that the classes in the legend of SSI-1 differ from SSI-6.

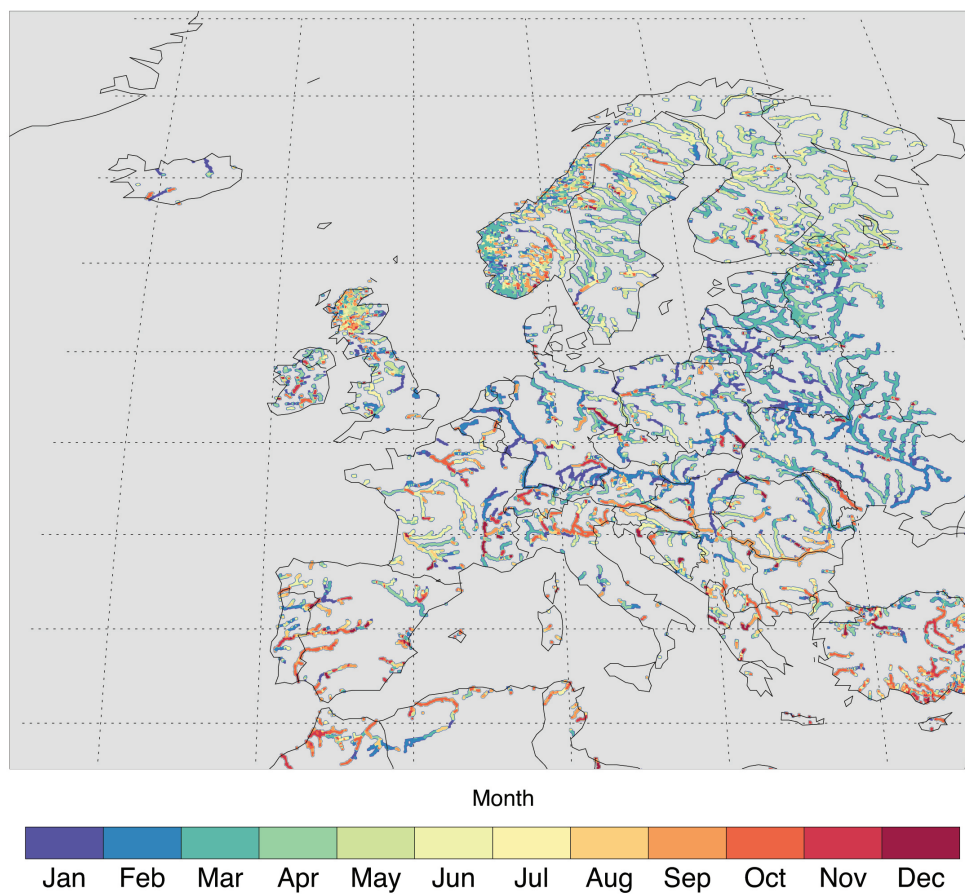


**Figure A2.** Months when drought mostly started in the European rivers from October 1990 to September 2018 identified using the SSI-1.